1-1-2001

Liquid crystal-based self-aligning 2 X 2 wavelength routing module

Sarun Sumriddetchkajorn

Nabeel A. Riza

Deepak K. Sengupta
University of Central Florida

Liquid crystal-based self-aligning 2×2 wavelength routing module

Sarun Sumriddetchkajorn
Nabeel A. Riza,* FELLOW SPIE
Deepak K. Sengupta
University of Central Florida
Photonics Information Processing Systems (PIPS) Laboratory
School of Optics
and
Center for Research and Education in Optics and Lasers (CREOL),
4000 Central Florida Boulevard
Orlando, Florida 32816-2700
E-mail: riza@creol.ucf.edu

Abstract. A novel retroreflective polarization insensitive 2×2 fiber optic switch (FOS) using programmable quarter waveplates (QWPs) is introduced. Key features include low polarization sensitivity and a self-aligning module via a compact retroreflective structure. A proof of concept 2×2 FOS using ferroelectric liquid crystal (FLC)-based programmable QWPs is demonstrated, providing a response speed of 394 μs and a low 10.14-mW total electrical power consumption for the worst case. Multiwavelength switch operation in the 1550-nm wavelength region indicates an average optical loss of 6.02 dB with a ±0.18-dB loss fluctuation, and an optical coherent crosstalk of −21.6 dB with a ±0.84 dB variation over a 60-nm bandwidth. The temperature dependence of our switch is investigated over a 17°C range, indicating an average 5.80-dB optical loss with a ±0.13-dB fluctuation, and an average optical coherent crosstalk of −20.5 dB with a fluctuation of ±0.42 dB. An average polarization dependent loss of 0.4 dB is also measured. A time-multiplexed FLC device addressing technique is introduced for FOS to achieve long duration operation. [DOI: 10.1117/1.1387988]

Subject terms: fiber optic switches; liquid crystal devices; electro-optic switches; optical interconnections; optical fiber communications.

Paper 200422 received Oct. 27, 2000; accepted for publication Mar. 30, 2001.

1 Introduction

Today, significant progress has been achieved in the design of high capacity, flexible, wide-bandwidth and scalable, wide-area multiwavelength optical networks.[1] A required key element is a reconfigurable multiwavelength add-drop multiplexer (ADM), in which the desired wavelength channels can be added into or dropped out of the wavelength division multiplexed (WDM) network at the specified locations. Multiwavelength ADMs with reconfigurable functions have been demonstrated using technologies such as integrated[2] and bulk[3] acousto-optic tunable filters (AOTFs), two-dimensional small tilt micromirrors,[4] fiber Bragg gratings,[5] and WDM demultiplexer/multiplexer interconnected device.[6] The ADM using WDM multiplexers needs fiber optic space switches to perform active add and drop operations. Hence, the performance of such an ADM depends on the qualities of the WDM multiplexer and the FOSs. Given the current maturity of WDM multiplexer technology, a key concern for building a WDM-based ADM is to realize a low cost, reliable, wavelength insensitive, and fast response time FOS. Previously, the most mature commercially available FOS was based on optomechanical movement.[7] For large scale network switching, these optomechanical switches have limitations such as low scalability, reliability issues due to physically moving parts, and in most cases, relatively slow (several milliseconds) switching times. Hence, it would be desirable to develop a FOS that can provide, in large part, similar attributes of an optomechanical switch but also overcome most of its limitations. Recently, a 2×2 FOS based on the combination of a Faraday rotator and a half waveplate (HWP) has been commercially developed.[8] However, this FOS requires a high 2.7-W electrical driving power to achieve a 1-ms switching speed and a 2-dB insertion loss. In addition, it provides a −30-dB optical coherent crosstalk with a ±5-dB fluctuation over a 60-nm bandwidth. Therefore, it would be highly desirable to have a FOS that requires a much lower electrical driving power that can provide a faster switching speed with small optical coherent crosstalk fluctuations for broadband operation. Low cost nematic liquid crystal (NLC) devices are an excellent choice for lower power consumption optical switch implementation,[9,10] although with response speeds limited to the millisecond regime. One way to achieve faster switching speeds and low power consumption is to use ferroelectric liquid crystal (FLC) devices. Previously, 35-μs switching speed 2×2 FOS modules were realized.[11,12] These FLC-based FOSs required careful optical alignment of several components.

We demonstrate the use of LC-based programmable quarter waveplates (QWPs) to realize a simple aligned compact 2×2 FOS structure.[13,14] Key features of our FOS includes low polarization sensitivity, low electrical power consumption, and a self-aligning module via a compact retroreflective structure. Section 2 describes how the LC-based programmable QWPs can be used to form our 2×2 FOS architecture. Section 3 gives the performance analysis of the FOS in terms of optical loss and optical coherent crosstalk. Section 4 gives the experimental data

*Also with Nuonics, Inc., Orlando, FL, www.nuonics.com

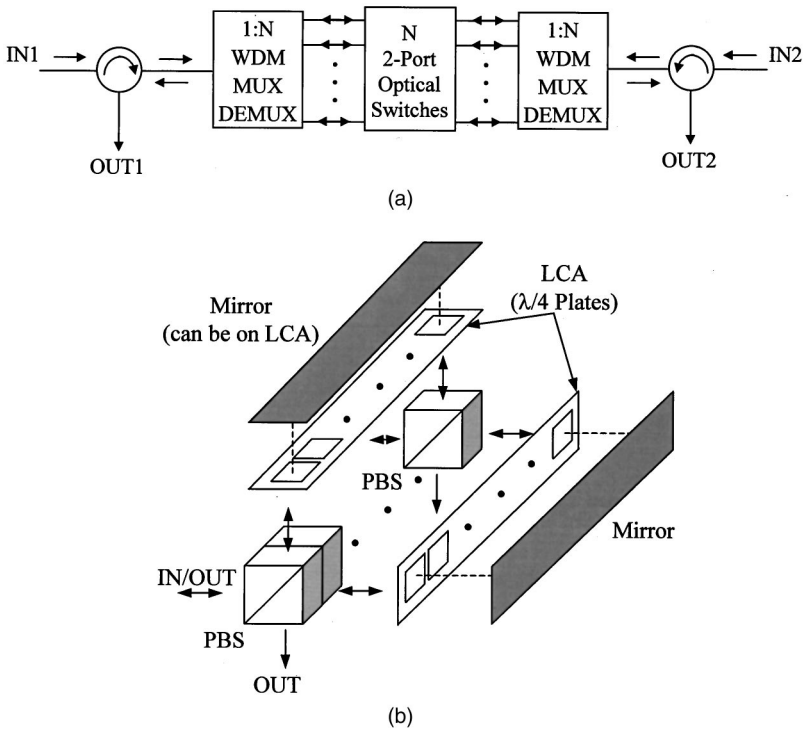

Fig. 1 (a) Proposed retroreflective add-drop multiplexer structure and (b) three-dimensional packaged view of our symmetric polarization insensitive two-port FOS structure.

for our FOS, including wavelength and temperature dependent tests, and polarization sensitivity. Section 5 concludes the paper.

2 Liquid Crystal-based Retroreflective 2×2 Fiber Optic Switch

Our retroreflective ADM structure is shown in Fig. 1(a). The reflective optical architecture rather than transmissive structure is selected because it reduces the required number of WDM multiplexers through the use of lower cost optical circulators.[15] In this architecture, the main multiwavelength optical signal beam is fed to the IN1 port, while the added multiwavelength optical beam enters at the IN2 port. After these two optical beams pass through the three-port optical circulators, they are demultiplexed by $1:N$ WDM demultiplexers, where N is the number of wavelength channels. The output ports of the WDM multiplexers are connected directly to the N symmetric two-port FOSs. Depending on the two-port FOS settings, the desired wavelength optical beams can be added into the OUT1 port or dropped at the OUT2 port. For example, if a two-port FOS is set such that the optical beams are sent back to their previous paths, there is no optical beam from the IN2 port added to the OUT1 port, and no optical beams from the IN1 port dropped at the OUT2 port. On the other hand, when the two-port FOS is programmed in such a way that the optical beams can be directed through the opposite direction, the add-drop operation occurs. Based on these operations, it is clear that the key component in this active ADM structure is the two-port FOS. Our implementation of the two-port FOS is shown in Fig. 1(b), indicating how compact low cost packaging can be implemented using LC panels. Our FOS is based on the combination of two polarization-dependent switching channels that form a polarization independent design, where one channel is for the vertical or *s*-polarized light and the other channel is for the horizontal or *p*-polarized light. A unique feature of our structure is the proper positioning and use of two LC devices, a 90-deg spatial split polarization beam splitter (PBS), and two mirrors that lead to a highly desirable self-aligning and low polarization sensitive symmetric reflective architecture. The PBS separates the incident optical beam into two orthogonal polarized beams with a 90-deg spatial deviation. The LC device used in this structure is designed to operate as a programmable QWP at the specified operating wavelengths. Note that any programmable QWP technology can be deployed in our FOS structure. This symmetric retroreflective two-port FOS structure offers the flexibility to feed the optical beam at either the IN1 or the OUT2 port. In other words, when this symmetric retroreflective two-port FOS structure is combined with two three-port optical circulators, a retroreflective 2×2 FOS can be formed. Figure 2 shows the two switching modes of operation of our FOS. When both LC devices are programmed to the ON state, as shown in Fig. 2(a), they represent QWPs orientated at an angle of 45 deg with respect to the directions of the electric fields of the linearly polarized optical beams emerging from the PBS. In this case, the linearly polarized light is converted into circularly polarized light, after traveling through the LC device. A mirror reflects the circularly polarized light back to the LC device, where this circularly polarized light is transformed back to a linearly polarized light of the orthogonal direction with respect to the linearly polarized input light. Hence, the *p*-and *s*-polarized optical beams are rotated 90 deg to become *s*- and *p*-polarized optical beams, respectively. Once these *s*- and *p*-polarized beams combine

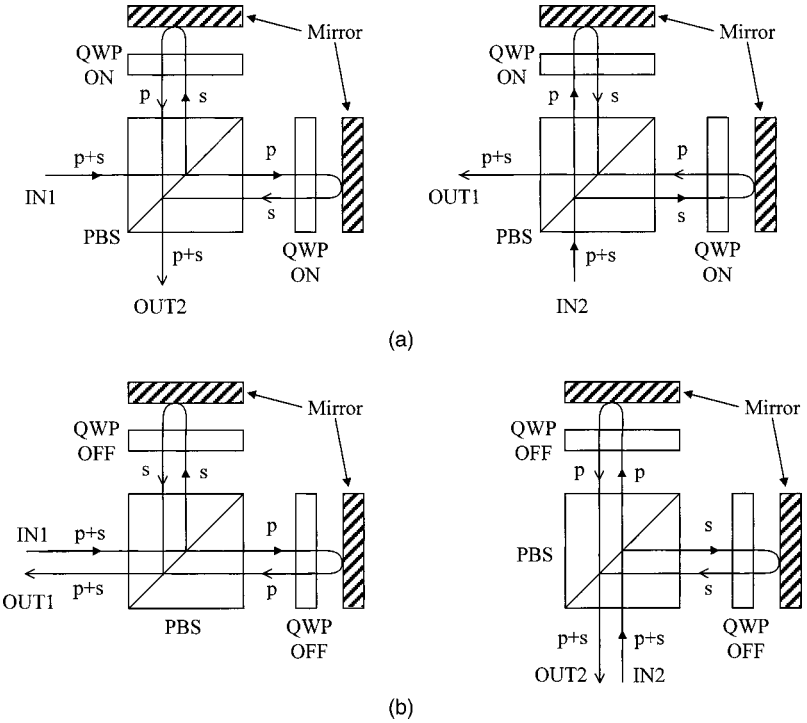

Fig. 2 The operation of our two-port FOS structure: (a) exchanging state and (b) straight state.

at the PBS, the optical beams from the IN1 and IN2 ports are sent to the OUT2 and OUT1 ports, respectively. On the other hand, when the LC devices are set to the OFF state, as shown in Fig. 2(b), the LCs act as nonbirefringent slab plates leading to no conversion of the input beam polarizations, indicating that the input optical beams are retroreflected to their own input ports.

It can be seen that the advantages of this retroreflective 2 $\times$2 FOS structure are: (a) the losses, i.e., the structure optical loss and the FOS polarization dependent loss (PDL) from both paths in the switch are balanced; (b) the optical delay paths of both switching states are the same, implying a low polarization mode dispersion (PMD); (c) the switch can be compact due to the small size of the planar thin film LC devices and the use of few components in a retroreflective structure; and (d) alignment and assembly of this FOS is simple and fast, leading to commercial viability.

3 Theoretical Analysis of Switch Loss and Interchannel Crosstalk Performances

In practice, a PBS does not entirely reflect the *s*-polarized light and transmit *p*-polarized light. In addition, any LC-based programmable QWP device does not convert a linearly polarized input light beam into a perfect circularly polarized output light beam. To analyze our 2×2 FOS performance, the specifications of each optical element used in the structure must be considered. These include the optical loss of each component and the polarization extinction ratios (PERs) of the PBS and LC devices.

3.1 *Architecture Loss Performance*

Optical loss in dB can be expressed as:

$$\text{Optical Loss} = L_{\text{cir}} + L_{\text{free-space}} + L_{\text{mirror}} + 2(L_{\text{adapter}} + L_{\text{PBS}} + L_{\text{LC}}), \quad (1)$$

where L_{cir}, $L_{\text{free-space}}$, L_{mirror}, L_{adapter}, L_{PBS}, and L_{LC} are the average optical losses in dB from the three-port optical circulators, free-space fiber-to-fiber coupling, mirrors, fiber adapters, the PBS, and LC devices, respectively. The L_{LC} depends on whether the LC devices are set to the ON or OFF state, and $L_{\text{free-space}}$ relies on the optical path length for each switch setting.

3.2 *Architecture Optical Coherent Crosstalk Performance*

The optical coherent crosstalk is defined as the ratio of the optical power in the noise wavelength at the unwanted switching port to the optical power in the signal wavelength at the desired switching port when the LC devices are ON (exchanging state) or OFF (straight state). The optical coherent crosstalk is caused by the imperfections of the LC devices and PBS, and the back reflection from the surfaces of the optical components. By assuming that all optical components are antireflection coated, the effect due to the back reflections is insignificant. For general analysis, the input optical beam is assumed to be linearly polarized at 45 deg. In this case, by calculating the optical power along the

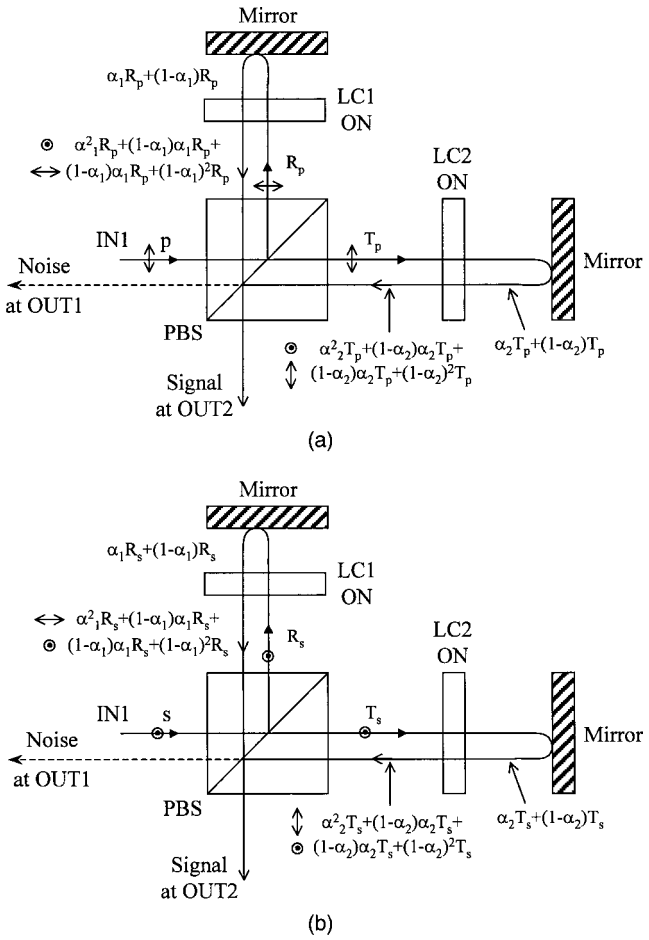

Fig. 3 The optical signal and optical noise flows in our LC-based two-port FOS when LC devices are set to the ON state for (a) *p*-polarized light and (b) *s*-polarized light.

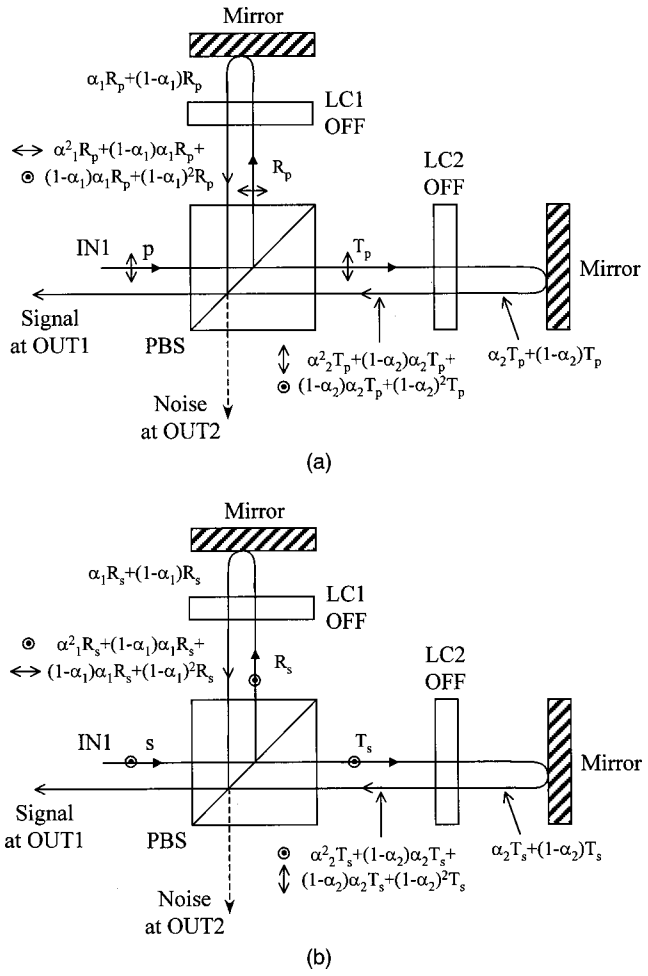

Fig. 4 The optical signal and optical noise flows in our LC-based two-port FOS when LC devices are set to the OFF state for (a) *p*-polarized light and (b) *s*-polarized light.

signal flow path and the noise power along the crosstalk flow path, we can derive the optical coherent crosstalk expressions in dB as:

$$\text{Crosstalk}=10\log\left(\frac{\text{Noise}_p+\text{Noise}_s}{\text{Signal}_p+\text{Signal}_s}\right), \tag{2}$$

where $(\text{Noise}_p, \text{Noise}_s)$ and $(\text{Signal}_p, \text{Signal}_s)$ are the optical noise powers and optical signal powers, respectively. The subscript indicates the specific light polarization. These optical powers can be found depending on the following cases.

Figure 3 shows the optical signal and optical noise flow patterns in our two-port FOS structure for *p*- and *s*-polarized lights, respectively. Here, both LC-based programmable QWP devices are set to the ON state and the optical beam is fed at the IN port. The expressions of optical signal power and optical noise power for the *s*- and *p*-polarized light beams can be written as

$$\text{Signal}_{p,\text{ON}}=2R_pT_p+\alpha_1a_p(b_s-b_p)+\alpha_2b_p(a_s-a_p), \tag{3}$$

$$\text{Noise}_{p,\text{ON}}=R_p^2+T_p^2+\alpha_1a_p(a_s-a_p)+\alpha_2b_p(b_s-b_p), \tag{4}$$

$$\text{Signal}_{s,\text{ON}}=2R_sT_s+\alpha_1a_s(b_p-b_s)+\alpha_2b_s(a_p-a_s), \tag{5}$$

$$\text{Noise}_{s,\text{ON}}=R_s^2+T_s^2+\alpha_1a_s(a_p-a_s)+\alpha_2b_s(b_p-b_s). \tag{6}$$

Here α_i $(i=1$ and $2)$ is the fraction of light that has its state of polarization (SOP) converted by the LC_i device. For example, if the $i=1$ LC device can transform a perfect circularly polarized light beam input to a linearly polarized light beam with a PER of 345:1, $\alpha_1=345/346=0.997$. R_s and R_p are the PBS reflectivities for the *s*- and *p*-polarized light beams, respectively. T_s and T_p are the PBS transmissivities for the *s*- and *p*-polarized light beams, respectively. a_s, a_p, b_s, and b_p are equal to R_s, R_p, T_s, and T_p, respectively. Note that a similar analysis method can be applied for the case of an optical beam fed at the IN2 port. In this case, a_s, a_p, b_s, and b_p are equal to T_s, T_p, R_s, and R_p, respectively.

Figure 4 shows the optical signal and optical noise flows in our two-port FOS structure for *p*- and *s* polarized lights, respectively, when both LC-based programmable QWP devices are set to the OFF state and the optical beam is fed at the IN1 port. In this way, the expressions of optical signal power and optical noise power for the *s*- and *p*-polarized lights can be written as

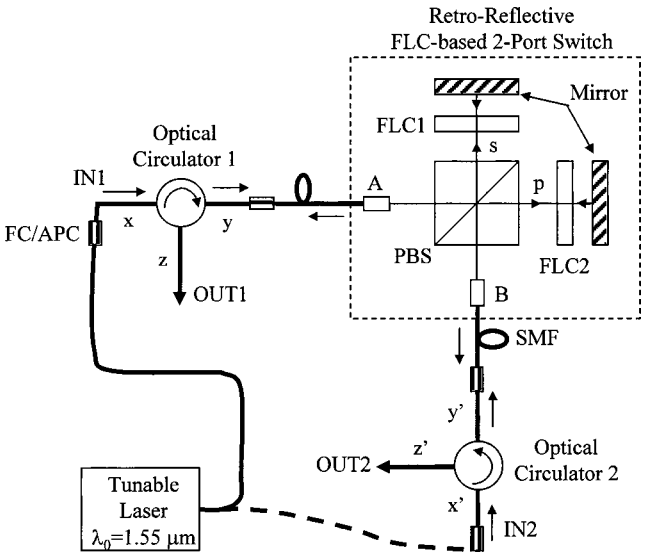

Fig. 5 LC-based 2×2 FOS experimental setup. SMF stands for single mode fiber.

$$\text{Signal}_{p,\text{OFF}} = R_s R_p + T_s T_p + \alpha_1 a_p (a_p - a_s) + \alpha_2 b_p (b_p - b_s), \tag{7}$$

$$\text{Noise}_{p,\text{OFF}} = R_p T_s + R_s T_p + \alpha_1 a_p (b_p - b_s) + \alpha_2 b_p (a_p - a_s), \tag{8}$$

$$\text{Signal}_{s,\text{OFF}} = R_s R_p + T_s T_p + \alpha_1 a_s (a_s - a_p) + \alpha_2 b_s (b_s - b_p), \tag{9}$$

$$\text{Noise}_{s,\text{OFF}} = R_p T_s + R_s T_p + \alpha_1 a_s (b - b_p) + \alpha_2 b_s (a_s - a_p), \tag{10}$$

Similar to the case of ON state LC devices, a_s, a_p, b_s, and b_p are equal to R_s, R_p, T_s, and T_p, respectively, for an optical beam fed at the IN1 port. If the optical beam is fed at the IN2 port, a_s, a_p, b_s, and b_p are equal to T_s, T_p, R_s, and R_p, respectively.

4 Experimental Demonstration of our LC-based Retroreflective 2×2 Fiber Optic Switch

The experimental setup of our LC-based 2×2 FOS is shown in Fig. 5. The FLC programmable QWP devices from Boulder Nonlinear Systems Incorporated, are designed to operate at 1550-nm wavelength. The FLC active pixel size diameter is 2 cm and is contained in a 4-cm-diam and 2-cm-thick package. The devices are driven with a ±10-V bipolar, dc-balanced (i.e., a 20 $V_{p\text{-}p}$) square wave signal. The frequency of the driving signal waveform is in the 0.5 Hz to 1 kHz range to prevent device failure. A +10 V with respect to the reference will place the device in the ON state, and a −10 V with respect to the reference will place the device in the OFF state. Two 25.4-mm-diam and 9.5-mm-thick dielectric mirrors designed for 1550 nm with a 255-nm bandwidth (>99% reflectivity)[16] are used in the experimental setup. A 1530 to 1590-nm tunable laser diode centered at 1550-nm wavelength is connected to either IN1 or IN2, with a FC/APC connector to determine our switch performance. All fiber optic components such as graded index (GRIN) fiber collimators and three-port optical circulators are also connected together via FC/APC connectors to reduce the return loss (e.g., <−60 dB).[17] A measured average optical path length from fiber to fiber is 19.95 cm. Using the fiber coupling analysis expression[18] for a 19.95-cm separation misalignment, a fiber coupling loss of 4.02 dB is calculated. The CCD images of the binary switch operation are shown in Fig. 6, where the input optical beam is fed at IN1. In this case, when FLC devices are set to the ON state, the optical beam from IN1 travels to OUT2 (see top image). On the other hand, the optical beam from IN1 appears at OUT1 (see bottom image) when FLC devices are set to the OFF state. The worst case FLC device switching time measured is 394 μs for FLC2 in our system.

The power consumption of each FLC device can be found as follows. Because the FLC device can be treated as a capacitive element, the required driving electrical power can be calculated as $\frac{1}{2}CV^2/T$ where C is the capacitance of the FLC device in farads, V is the peak electrical driving voltage in volts, and T is the charging time of the FLC device in seconds. For our FLC devices, the required driving voltage is ±10 V and the measured capacitances of FLC1 and FLC2 are 39 nF and 41 nF, respectively. With the worst case FLC charging time of 394 μs, the electrical power consumption of the FLC1 and FLC2 are 4.94 and 5.20 mW, respectively, indicating a 4.94+5.20 =10.14 mW total electrical power required to operate our 2×2 FOS.

Although the FLC-based switch can provide a reasonable response speed with a very low electrical power consumption, a present limitation of FLCs is that the voltage polarity of the FLC device driving signal must be changed after some time, e.g., <2 sec.[19] Time multiplexed FLC device addressing can solve this problem. In this case, two cascaded QWP FLC devices replace the one QWP FLC device in the original design. For switch exchanging state operation, the two cascaded FLC devices are inversely operated in polarity, so that we have only one QWP at a time. On the other hand, when all FLC devices are set simultaneously to ON and OFF states, implying the same polarity drive, the switch works in the straight state. This is because when all FLC devices are in the ON state, the overall wave retarder is a HWP rather than a QWP. Therefore, once the optical beam split by the PBS has returned back to the PBS, its input linear SOP has a 180-deg polarization direction flip, and still is linear. In addition, when all FLC devices are in the OFF state, they act is nonbirefringent glass plates and there is no SOP change in the optical beam.

The multiwavelength performance of our 2×2 FOS structure is also investigated at 23°C, our laboratory room temperature. Figure 7(a) shows the measured optical loss versus operating wavelength, indicating an average optical loss of 6.02 dB with a ±0.18-dB fluctuation over a 60-nm bandwidth. From Table 1, it is clear that this optical loss value comes from two three-port optical circulators (L_{cir} =1.21 dB), two fiber adapters ($2L_{\text{adapter}}$=0.60 dB), a round-trip PBS ($2L_{\text{PBS}}$=0.32 dB), two dielectric mirrors ($2L_{\text{mirror}}$=0.04 dB), and a round-trip via the FLC devices ($2L_{\text{LC}}$=0.31 dB). With these factors and using Eq. (1), a fiber-to-fiber coupling loss ($L_{\text{free-space}}$) of 3.54 dB is calcu-

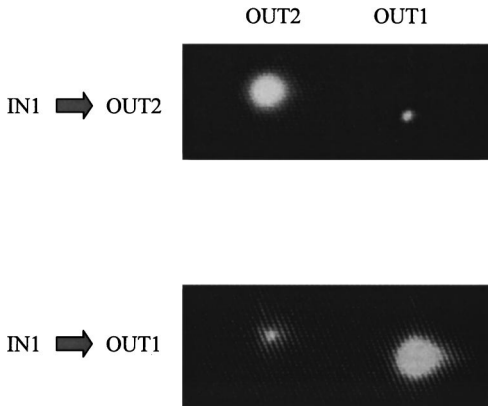

Fig. 6 CCD images of the binary switch operation for which the input optical beam is fed at IN1 port.

lated. This fiber-to-fiber coupling loss number is 0.48 dB less than the 4.02 dB derived from the formula in Ref. 18. Lower optical loss can be achieved by optimizing the fiber coupling distance, using lower loss PBS, three-port optical circulators, and FLC devices, and using fusion splices instead of fiber adapters.

Another important system issue is the optical coherent crosstalk. Using Eqs. (2)–(10) derived in Sec. 3 and the measured specifications of components listed in Table 1, an average −20.85 dB optical coherent crosstalk is calculated for a 1550-nm operation. The measured optical coherent crosstalk of our 2×2 FOS experimental setup is shown in Fig. 7(b), indicating an average −21.6-dB optical coherent

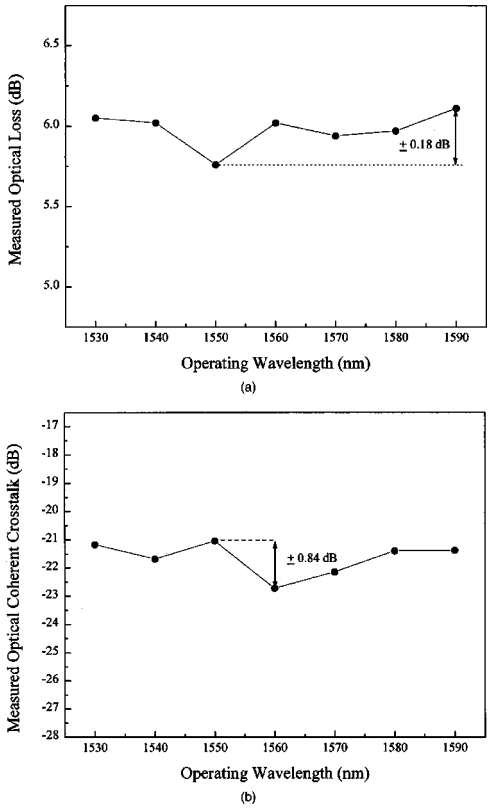

Fig. 7 FLC-based 2×2 FOS multiwavelength operation test: (a) the measured optical loss versus operation wavelength and (b) the measured optical coherent crosstalk versus operating wavelength.

Table 1 Specifications of the optical components used in our FLC-based 2×2 FOS experimental setup. Note that *p* and *s* stand for *p*- and *s*-polarized lights, respectively.

Components	Specifications	Operating Temperature/Vendor
Dielectric mirror	$R>99\%$	−10 to 250°C with the rate of temperature change <5–10°C/hr (CVI Corp., USA)
PBS	$R_p=0.109\%$, $R_s=99.930\%$ $T_p=99.891\%$, $T_s=0.070\%$ Optical Loss: 0.16 dB	−50 to 90°C (NewPort Corp., USA)
Optical circulator 1	Optical Loss: $x\rightarrow y=0.53$ dB $y\rightarrow z=0.65$ dB	0 to 65°C (Kaifa Technology, Inc., USA)
Optical circulator 2	Optical Loss: $x'\rightarrow y'=0.59$ dB $y'\rightarrow z'=0.64$ dB	0 to 65°C (Kaifa Technology, Inc., USA)
FLC1	PER: 345:1	5 to 55°C
	Optical Loss: 0.16 dB (ON) 0.11 dB (OFF)	(Boulder Nonlinear Systems, Inc., USA)
FLC2	PER: 100:1	5 to 55°C
	Optical Loss: 0.20 dB (ON) 0.16 dB (OFF)	(Boulder Nonlinear Systems, Inc., USA)
FC/APC adapter	Optical Loss: 0.28 dB	-
Single mode fiber	Optical Loss: 0.2 dB/km	−60 to 85°C (Corning Inc., USA)
Fiber collimator	-	−15 to 55°C (OZ Optics, Ltd. Canada)

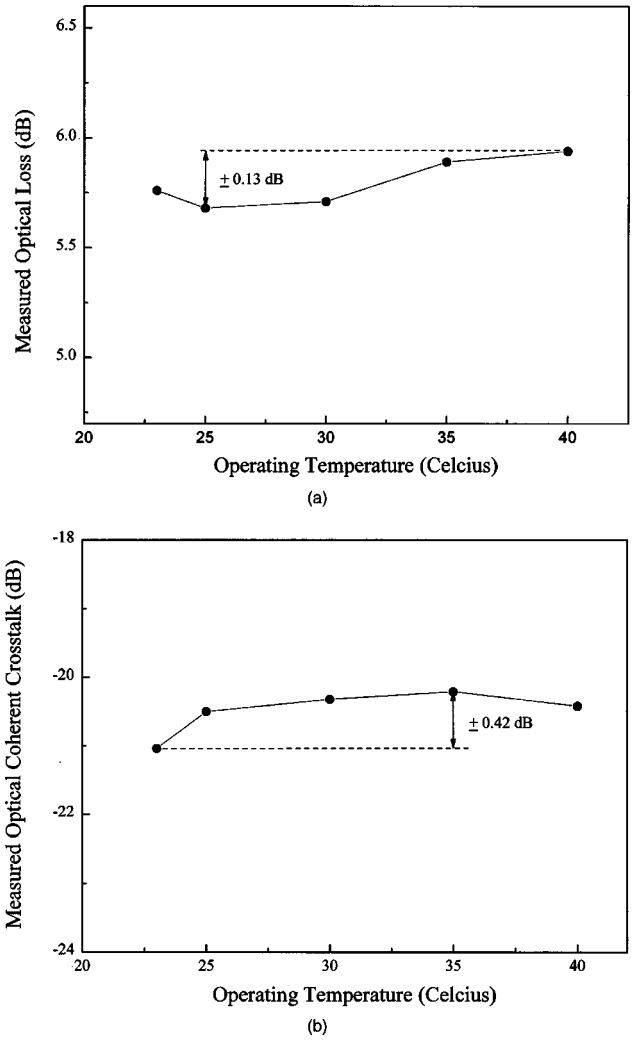

Fig. 8 FLC-based 2×2 FOS temperature dependent test results: (a) the measured optical loss versus operating temperature and (b) the measured optical coherent crosstalk versus operating temperature.

crosstalk with a ±0.84-dB fluctuation over a 60-nm bandwidth. In particular, the measured optical coherent crosstalk at 1550 nm is −21.04 dB, which is consistent with the expected value. The optical coherent crosstalk is limited by the PERs of the PBS and the FLC devices used in our structure. With a typical NLC device 1000:1 PER, the same experimental switch will give an expected optical coherent crosstalk of <−25.5 dB, corresponding to the standard requirement for telecom fiber optic switches.[20] Similarly, any PBS with a better PER will improve crosstalk.

PDL and PMD can be used to indicate our 2×2 FOS polarization-dependent behavior. To investigate the PDL in our FOS structure, a fiber-based polarization controller is inserted between the tunable laser diode and the input port (e.g., port x or port x' in Fig. 5) of the three-port optical circulator to scramble the SOP of the input optical beam. In this way, an average PDL of 0.40 dB is measured. This PDL comes from the unbalanced optical loss of the two polarization independent switching channels and three-port optical circulators used in our FOS structure. The PMD in our FOS can be simply estimated by considering the optical path length difference traveled by the *p*- and *s*-polarized optical beams, i.e., the difference in distance between the PBS and the two dielectric mirrors. Based on the experimental setup shown in Fig. 5, the measured round-trip optical path difference between two orthogonal polarized optical beams is $2\times0.3=0.6$ mm, indicating a 2-ps PMD in our FOS experimental setup. PMD reduction can be accomplished by optimizing the optical path length difference.

Temperature testing of the FOS on the optical table is implemented by covering the experimental setup with a stainless steel sheet and placing two heaters inside the enclosure. To get closed-loop feedback control, a thermocouple from the heater controller is hung above the PBS, which is near the center position of our FOS structure. With this setup, we observe that the temperature can be stabilized at a desired temperature setting for more than an hour. Based on this uncovered temperature test setup and the operating temperature range of each optical component (see Table 1), our FOS performance is investigated for a 23°C room temperature to 40°C. Figure 8(a) shows the measured optical loss versus operating temperature, indicating an average 5.80-dB loss with a ±0.13-dB fluctuation. The measured optical coherent crosstalk is also shown in Fig. 8(b), indicating an average optical coherent crosstalk of −20.5 dB with a ±42-dB fluctuation.

5 Conclusion

We have presented a novel 2×2 FOS architecture using programmable QWP devices. Our 2×2 FOS structure can offer not only low polarization sensitivity but also a self-aligning switch module using a compact retroreflective design. With FLC-based programmable QWP devices, a worst case 394-μs switching time is measured with a low 10.14 mW total electrical power consumption. A time multiplexed FLC device addressing technique with a few hertz modulation is proposed to obtain long time duration stable switch operation. Experimental results show an average −21.6-dB optical coherent crosstalk with a ±0.84-dB fluctuation and an average optical loss of 6.02 dB with a loss fluctuation of ±0.18 dB over a 60-nm bandwidth. The switch temperature dependence is also investigated, indicating an average optical loss of 5.80 dB with a loss fluctuation of ±0.13 dB, and an average −20.5-dB crosstalk with ±0.42-dB fluctuation. A measured PDL of 0.40 dB and a 2-ps PMD is delivered by the FOS. Immediate <−25-dB crosstalk improvements are possible using NLC QWPs.

References

1. R. E. Wagner, R. C. Alferness, A. A. M. Saleh, and M. S. Goodman, "MONET: Multiwavelength optical networking," *J. Lightwave Technol.* **14**(6), 1349–1355 (June 1996).
2. D. A. Smith, J. E. Baran, J. J. Johnson, and K. W. Cheung, "Integrated-optic acoustically tunable filters for WDM networks," *IEEE J. Sel. Areas Commun.* **8**(6), 1151–1159 (Aug. 1990).
3. N. A. Riza and J. Chen, "Ultra-high −47 dB optical drop rejection multi-wavelength add-drop filter using spatial filtering and dual bulk acousto-optic tunable filters," *Opt. Lett.* **23**(12), 945–947 (June 1998).
4. N. A. Riza and S. Sumriddetchkajorn, "Fault-tolerant dense multi-wavelength add-drop filter with a two-dimensional digital micromirror device," *Appl. Opt.* **37**(27), 6355–6361 (Sept. 1998).
5. H. Okayama, Y. Ozeki, and T. Kunii, "Dynamic wavelength selective add/drop node comprising tunable gratings," *Electron. Lett.* **33**(10), 881–882 (May 1997).
6. K. Okamoto, K. Takiguchi, and Y. Ohmori, "16-channel optical add-drop multiplexer consisting of arrayed-waveguide gratings and double-gate switches," *Electron. Lett.* **32**(16), 1471–1472 (Aug. 1996).

7. M. S. Borella, J. P. Jue, B. Ramamurthy, and B. Mukherjee, ''Optical components for WDM lightwave networks,'' *Proc. IEEE* **85**(8), 1274–1307 (1997).
8. Product Catalog, *Optical Switch YS-111 Type*, FDK Corp. (1998).
9. R. A. Soref, ''Low-cross-talk 2×2 optical switch,'' *Opt. Lett.* **6**(6), 275–277 (1981).
10. N. A. Riza, ''High-optical-isolation low-loss moderate-switching-speed nematic liquid-crystal cells,'' *Opt. Lett.* **19**(21), 1780–1782 (1994).
11. N. A. Riza and S. Yuan, ''Low optical interchannel crosstalk, fast switching speed, polarization independent 2×2 fiber optic switch using ferroelectric liquid crystals,'' *Electron. Lett.* **34**(13), 1341–1342 (1998).
12. N. A. Riza and S. Yuan, ''Reconfigurable wavelength add-drop filtering based on a Banyan network topology and ferroelectric liquid crystal fiber-optic switches,'' *J. Lightwave Technol.* **17**(9), 1575–1584 (Sept. 1999).
13. N. A. Riza, ''Ferroelectric liquid crystal polarization switching-based high speed multiwavelength add/drop filters using fiber and array waveguide gratings,'' *Proc. SPIE* **3490**, 335–338 (June 1998).
14. S. Sumriddetchkajorn, D. K. Sengupta, and N. A. Riza, ''Self-aligning 2×2 fiber-optic switch using liquid crystal,'' *IEEE LEOS Annual Meeting*, San Francisco, Vol. 1, pp. 135–136 (Dec. 1999).
15. S. Sumriddetchkajorn, ''Fiber-optic beam control systems using microelectromechanical systems (MEMS),'' PhD Dissertation, University of Central Florida (2000).
16. Technical data, CVI Laser Corp. (1997).
17. Product Catalog, Wave Optics, Inc. (1999).
18. S. Yuan and N. A. Riza, ''General formula for coupling-loss characterization of single-mode fiber collimators by use of gradient-index rod lenses,'' *Appl. Opt.* **38**(15), 3214–3222 (May 1999); Erratum, *Appl. Opt.* **38**(30), 6292 (Oct. 1999).
19. J. Stockley, Boulder Nonlinear Systems, Inc., 450 Courtney Way, Unit #107, Lafayette, CO 80026, Private Communication.
20. TR-NWT-001073: *Generic Requirements for Fiber Optic Switches*, Bellcore, Issue 1, (Jan. 1994).